

Practical time-delay synchronization of a periodically modulated self-excited oscillators with uncertainties

F. M. Moukam Kakmeni,^{1,a)} S. Bowong,^{2,3} D. V. Senthikumar,^{3,4} and J. Kurths^{3,5}

¹Laboratory of Research on Advanced Materials and Nonlinear Science (LaRAMaNS), Department of Physics, Faculty of Science, University of Buea, P.O. Box 63, Buea, South-West 237, Cameroon

²Laboratory of Applied Mathematics, Department of Mathematics and Computer Science, Faculty of Science, University of Douala, 24157 Douala, Cameroon

³Potsdam Institute for Climate Impact Research, 14473 Potsdam, Germany

⁴Centre for Dynamics of Complex Systems, 14469 Potsdam Germany

⁵Institute of Physics, Humboldt University, 12489 Berlin, Germany

(Received 3 March 2010; accepted 24 October 2010; published online 22 November 2010)

This paper studies time-delay synchronization of a periodically modulated Duffing Van der Pol (DVP) oscillator subjected to uncertainties with emphasis on complete synchronization. A robust adaptive response system is designed to synchronize with the uncertain drive periodically modulated DVP oscillator. Adaptation laws on the upper bounds of uncertainties are proposed to guarantee the boundedness of both the synchronization error and the estimated feedback coupling gains. Numerical results are presented to check the effectiveness of the proposed synchronization scheme. The results suggest that the linear and nonlinear terms in the feedback coupling play a complementary role in increasing the synchronization regime in the parameter space of the synchronization manifold. The proposed method can be successfully applied to a large variety of physical systems. © 2010 American Institute of Physics. [doi:10.1063/1.3515840]

Synchronization phenomena of chaotic systems are of fundamental importance and have been observed in nature and science. They have been widely investigated for two decades, and many effective methods have been presented. Recently, chaos synchronization phenomena of coupled chaotic self-sustained systems have attracted much attention, since their well-controllable parameters and their well-studied nonlinear behavior make them ideally suited for studies of the fundamental synchronization phenomena of coupled nonlinear systems. Such systems are of interest for technological applications in industry and for the understanding of biological processes involving self-sustained behavior, since the synchronization scenario related to variations of the system parameters is of high relevance for both aspects. Due to the simple configuration and easy implementation, unidirectional linear error feedback coupling scheme was adopted in many real systems. Also, time-delay systems have attracted a lot of attention in recent years, in part due to finite signal transmission times, switching speeds, and memory effects. Therefore, the study of synchronization phenomena in such systems is of high practical importance. In the present paper, we develop a practical synchronization method for self-sustained systems using an adaptive output nonlinear feedback coupling in the presence of time-delay, uncertainties, and external disturbances. Numerical simulations suggest that the linear and nonlinear terms in the feedback coupling play a complementary role for the improvement of the stability of the syn-

chronization manifold. These results are of significant interest to infer relationships between parameter mismatches, nonlinear feedback coupling, time-delay, and synchronization.

I. INTRODUCTION

Chaotic synchronization is one of the fundamental nonlinear phenomena actively studied recently,¹ having both important theoretical and applied significance, e.g., for information transmission by means of deterministic chaotic signals, in biology and physiology, for controlling lasers and microwave systems etc. (cf. Refs. 1–10 for review). Since the Volterra predator-prey model,¹¹ time-delay has been considered in various forms to incorporate realistic effects, e.g., distributed, state-dependent, and time-dependent time-delay. Up to now, the effects of these forms of delay in dynamical systems have been extensively studied in many fields of physics,¹² biology,¹¹ and economy.¹³ On the other hand, in many real situations, a time-delay is inevitable, as the propagation speed of the information signal is finite.¹⁰ Strictly speaking, in experimental situations with signal propagation delays, it is not reasonable to expect the response system to synchronize with the drive system at exactly the same time. It is similar to the telephone communication systems, where one hears the voice at time t on the receiver side, although it was uttered on the transmitter side some time earlier, say, at time $t - \tau$. Time-delayed systems are also interesting from the theoretical perspective because the dimension of their chaotic dynamics can be made arbitrarily large by increasing their delay-time.^{14,15} In this regard, it is important to understand synchronization of chaotic oscillators with time-delay.

^{a)} Author to whom correspondence should be addressed. Electronic mail: moukamkakmeni@gmail.com and fmoukam@yahoo.com.

Additionally, uncertainties occur commonly in many real-world control systems.^{13,16,17} It has been noted that when chaotic synchronization is applied to engineering such as communications, these chaos-based synchronization schemes are rather sensitive to noise and distortions in channels. This is an undesirable feature, as it is one of the main factors leading to a failure of the intended synchronization. This effect should be taken into account when we want to evaluate the performance of a practical chaos synchronization scheme. Furthermore, for chaos synchronization of uncertain dynamical systems, the bounds on uncertainties are important parameters and may not be easily obtained due to several causes. Therefore, adaptive methods must be employed to estimate such bounds. At present, little attention has been given to adaptive synchronization between coupled chaotic systems without the limitation of knowing the bounds of uncertainties.

Many studies on chaos synchronization have been derived on the basis of a linear feedback coupling has been limited to the assumption of linear feedback coupling.^{16,18–22} However, the implementation of feedback coupling of practical systems is frequently subject to nonlinearities as a result of physical limitation. Their presence may lead to serious degradation of the system's performance, decrease in speed of response, and may possibly cause perturbation of the originally regular behavior if the feedback coupling is not well designed. In addition, in those works, the design of the feedback coupling is limited to systems with full state feedback. In practical applications, a full measurement of the state might be neither possible nor feasible. Also, the only available information is the measured system's output, which represents a function of some current linear states of the system. Usually, the dimension of the vector measured signals is smaller than the dimension of the corresponding vector of states.

This paper studies an adaptive time-delay synchronization of a chaotic periodically modulated Duffing Van der Pol (DVP) oscillator subjected to uncertainties and channel time-delay in the drive-response framework. We will investigate adaptive synchronization of chaotic systems using an output nonlinear feedback coupling in the presence of a delay and uncertainties including parametric perturbations, modeling errors, time lag, and external disturbances. In the drive system, not only are the Lipschitz constants on function matrices and the bounds on uncertainties unknown but also the time-delay. A robust adaptive response system will be designed to practically synchronize the given driven periodically modulated DVP oscillator. Adaptation laws are chosen to estimate the unknown bounds of uncertainties and to repress external disturbances. These results are of significant interest to infer relationships between parameter mismatches, nonlinear feedback coupling, time-delay, and synchronization.

To the best of author's knowledge, adaptive synchronization of chaotic systems using an adaptive output time-delay nonlinear feedback coupling is to be investigated yet. Having in mind enormous implications of the application of chaos synchronization, investigation of synchronization regimes (lag, complete, etc.) in adaptive nonlinear time-delay

feedback coupling is of immense importance.

The outline of this paper is as follows. In Sec. II, we recall the dynamics of the periodically modulated self-excited oscillator. Then, we present the adaptive time-delay synchronization scheme in Sec. III. We use the Lyapunov stability theory to ensure the practical synchronization between the drive and response chaotic systems, whereby the Lipschitz constants on function matrices and the bounds on uncertainties as well as the time-delay are unknown. In Sec. IV, we give a stability analysis of the proposed adaptive time-delay synchronization scheme. Numerical simulations are presented in Sec. V to demonstrate the effectiveness of the proposed adaptive time-delay synchronization approach. The case of different time-delays in the nonlinear terms of the feedback coupling is also investigated. Finally, in Sec. V, concluding remarks are given.

II. DYNAMICS OF THE DVP OSCILLATOR

Herein, we consider the DVP oscillator.^{23–27} The dynamical variables is x and the equations read

$$\ddot{x} + \xi_i(t)x - \xi_{ii}(t)\dot{x} + \beta x^3 + \gamma x^2\dot{x} = \xi(t), \quad (1)$$

where $\xi_i(t) = \mu(1 + \varepsilon \cos \omega t)$, $\xi_{ii}(t) = \nu(1 + \varepsilon \cos \omega t)$, and μ , ν , γ , ω , β , and ε are positive parameters. Physically, ν and γ can be regarded as the dissipation or damping parameters, β is the strength of nonlinearity, ε and ω are the amplitude and frequency of the driving forces, respectively, and $\xi(t)$ is an external disturbance which may be considered as noise. Very recently, dynamical model (1) was used to describe the motor pathway in oscine birds. Part of this pathway is the nucleus RA (robustus nucleus of the archistriatum) containing excitatory neurons, some of which enervate respiratory nuclei and others enervate the nucleus nXIIts, which projects to the muscles in the syrinx (Refs. 24–26 and references therein).

We summarize the influence of the parametric forcing on the chaotic regime of the periodically modulated self-excited oscillator of Eq. (1). Figure 1 represents the bifurcation diagram of the system as a function of the parameters ε and β . These dynamics are determined by calculating the maximum Lyapunov exponent λ_{\max} as a function of the two main forcing parameters ε and β . In parameter ranges pertaining to the darker (blue) regions ($\lambda_{\max} = 0$), a quasiperiodic behavior is found. Gray (blue) regions ($\lambda_{\max} > 0$) correspond to chaotic dynamical states. Regions colored in light gray (blue) shades ($\lambda_{\max} < 0$) correspond to periodic motions. The (ε, β) space is characterized by the predominance of periodic motions. For low values of ε and high values of β , chaotic states are abundant. Also, one can find a band of quasiperiodic motion for smaller values of ε . When both parameters are increasing, the parameter space exhibits a more complex pattern whose chaotic regions appear side by side with a periodic regionlike fingers. Hence, the system generates qualitative changes for parameter variation. For slight variation in the parameters, the system can switch from a chaotic motion to a periodic one and vice versa. These complex dynamics justify the choice of this system as an illustrative example for the development of an adaptive time-delay synchronization algorithm in Sec. IV.

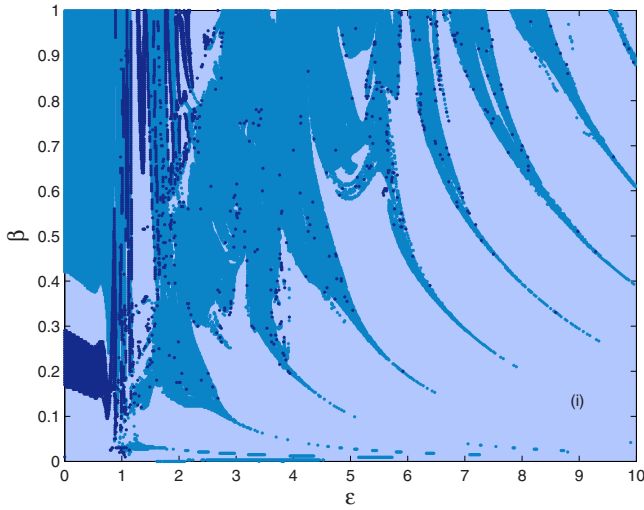


FIG. 1. (Color online) The domains of periodic, quasiperiodic, and chaotic solutions in the two-parameters diagram (ε, β) for $\nu=0.401, \mu=1.0434, \gamma=0.1, \omega=1, \xi(t)=0$. This diagram is determined numerically by finding the largest Lyapunov exponent of the system. In parameter ranges pertaining to the darker (blue) regions ($\lambda_{\max}=0$), quasiperiodic behaviors are found. Gray (blue) regions ($\lambda_{\max}>0$) correspond to chaotic dynamical states. Regions colored in light gray (blue) shades ($\lambda_{\max}<0$) correspond to periodic motions.

III. ADAPTIVE TIME-DELAY SYNCHRONIZATION ALGORITHM

In this section, we investigate the adaptive time-delay synchronization problem of coupled periodically modulated DVP oscillators with uncertainties and channel time-delay in the drive-response framework. By adaptive control, we mean a special type of a nonlinear control system which can alter its parameters to adapt to a changing environment. The changes in environment can represent variations in the process dynamics or changes in the characteristics of the disturbances. In other words, adaptive control is the capability of the system to modify its own operation to achieve the best possible mode of operation. We use the solution x of system (1) as the signal to be transmitted to the response system, i.e., $y=\dot{x}$. By changing the variables $x_1=x$ and $x_2=\dot{x}$, periodically modulated DVP oscillator (1) can be rewritten in a compact form as

$$\begin{cases} \dot{z} = A(\alpha)z + B[f(z, \alpha) + \xi(t)] \\ y = Cz, \end{cases} \quad (2)$$

where $z=(x_1, x_2)^T$ is the state, y is the output (measured variable), $\alpha=(\mu, \nu, \varepsilon, \beta, \gamma)^T$ is the parameter vector, $f(z, \alpha) = -\varepsilon\mu x_1 \cos \omega t + \varepsilon\nu x_2 \cos \omega t - \beta x_1^3 - \gamma x_2 x_1^2$ is the nonlinear part of Eq. (1), and $\xi(t)$ is the external perturbation,

$$A(\alpha) = \begin{bmatrix} 0 & 1 \\ -\mu & \nu \end{bmatrix}, \quad B = \begin{bmatrix} 0 \\ 1 \end{bmatrix}, \quad \text{and} \quad C = [0, 1].$$

The goal of this paper is to propose a scheme to solve the adaptive synchronization problem for system (2). That is to say, if uncertain system (2) is regarded as the drive system, a suitable response system should be constructed to synchronize with the drive system with the help of the driving signal y . In order to do so, we assume the following.

- (i) There is a bounded region $\mathcal{U} \subset R^2$ containing the whole basin of drive system (2) such that no orbit of system (2) ever leaves it.

Thus, the divergence of system (2) can be defined in an arbitrarily small time interval, because the initial infinitesimal distance between the solutions (2) become finite during the small interval ΔT_0 . It should be pointed out that in the classical case when a Lipschitz condition is satisfied, the distance between two diverging solutions can become finite only at $t \rightarrow \infty$ if initially this distance was infinitesimal. Further, the uncertain parameter vector α and the external disturbance vector $\xi(t)$ are norm bounded by two unknown positive constants α_m , and ξ_m , namely $\|\alpha\| \leq \alpha_m$ and $\|\xi\| \leq \xi_m$.

- (ii) Let $\mathcal{M} \subset R^5$ be a region containing the relevant parameter values for which system (2) exhibits a chaotic behavior. The matrix $A(\alpha)$ and the nonlinear function $f(z, \alpha)$ satisfy the following Lipschitz conditions:

$$\|A(\alpha) - A(\hat{\alpha})\| \leq k_a \|\alpha - \hat{\alpha}\|, \quad \forall \alpha, \hat{\alpha} \in \mathcal{M}, \quad (3)$$

$$|f(z, \alpha) - f(\hat{z}, \alpha)| \leq k_{f_1} |x_1 - \hat{x}_1| + k_{f_3} |x_1 - \hat{x}_1|^3, \quad (4)$$

$$\forall x_1, \hat{x}_1 \in \mathcal{U},$$

$$|f(z, \alpha) - f(z, \hat{\alpha})| \leq k_\alpha \|\alpha - \hat{\alpha}\|, \quad \forall \alpha, \hat{\alpha} \in \mathcal{M}, \quad (5)$$

where k_a , k_{f_1} , k_{f_3} , and k_α are positive constants.

The Lipschitz properties are satisfied locally if $A(\alpha)$ is differentiable with respect to α . The following analysis will remain valid if Eq. (2) is satisfied locally for $z \in \mathcal{U}$ and $\alpha \in \mathcal{M}$. Note also that the Lipschitz constants k_a , k_{f_1} , k_{f_3} , and k_α are often needed to be known for control design purposes. However, it is often difficult to obtain the precise values of k_{f_1} , k_{f_3} , and k_α in practical systems. Hence, the Lipschitz constants are often selected to be larger. This causes the feedback gains to be higher, and the results obtained are then very conservative.

- (iii) There exists a constant vector $L \in R^2$ to make the transfer function $H(s) = C(sI_2 - (A(\alpha) - LC))^{-1}B$ be strictly positive.

Finding a constant vector L satisfying (iii) is not a trivial task. However, it was shown in Refs. 13 and 17 using the Kalman–Yakubovich–Popov lemma that there exist two positive definite matrices $P=P^T$ and $Q=Q^T$ with appropriate dimensions such that the following algebraic equations hold:

$$(A(\alpha) - LC)^T P + P(A(\alpha) - LC) = -Q \quad (6)$$

and

$$B^T P = C. \quad (7)$$

Equation (7) implies that the span of rows of $B^T P$ belongs to the span of the rows of C . We point out that the transfer function is commonly used in the analysis of single-input single-output filters. This function is typically used to prove that the linear part of a nonlinear control system is

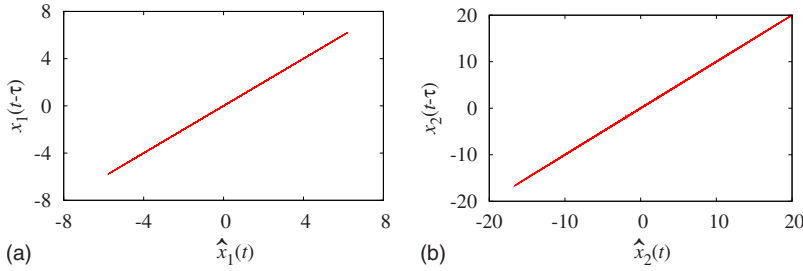


FIG. 2. (Color online) Relation between the drive and response systems under the feedback coupling when $\theta_1 = \theta_3 = 1$, $\varphi = 0.01$, and $\tau = 0.1$.

stable. Indeed, when this function is strictly positive, then all the eigenvalues of the matrix of the linear part of a nonlinear control system have negative real parts.

If the Lipschitz constants on $A(\alpha)$ and $f(z, \alpha)$ exist and the upper bounds of the uncertain parameter α and the uncertainty $\xi(t)$ are known, i.e., $k_a, k_{f_1}, k_{f_3}, k_\alpha, \alpha_m$, and ξ_m are given *a priori*, then a robust adaptive response system can be designed to overcome the effect of unknown parametric perturbations and unknown external disturbances and further to achieve synchronization. However, the main problem is that $k_a, k_{f_1}, k_{f_3}, k_\alpha, \alpha_m$, and ξ_m are unknown.

Taking the time-delay explicitly into account, the response system based on chaotic drive system (2) can be described as follows:

$$\begin{cases} \dot{\hat{z}} = A(\hat{\alpha})\hat{z} + B[f(\hat{z}, \hat{\alpha}) + \hat{\xi}(t)] + Bu(t - \tau) \\ \hat{y} = C\hat{z}, \end{cases} \quad (8)$$

where \hat{z} is the state, \hat{y} the output, $\hat{\alpha}$ is the parameter vector which is assumed to be different from $\alpha \in \mathcal{M}$, $\hat{\xi}(t)$ is the external disturbance, τ is a finite time-delay which is an unknown constant, and $u(t - \tau)$ is the feedback coupling, which will be designed so as to achieve synchronization between the drive and response systems (2) and (8).

Without the requirement of the information of the bounds of uncertainties, the objective is to design a nonlinear adaptive time-delay feedback coupling $u(t - \tau)$, such that the solutions of drive system (2) practically synchronize completely with the solution of response system (8), i.e.,

$$\|z(t - \tau) - \hat{z}\| \leq c, \quad t \rightarrow \infty, \quad (9)$$

where c is the error bound which can be made sufficiently small. This means that the synchronization is uniformly ultimately bounded.

To perform objective stated above, we propose the following adaptive nonlinear time-delay feedback coupling:

$$u(t - \tau) = \hat{\delta}_1(y(t - \tau) - \hat{y}) + \hat{\delta}_3(y(t - \tau) - \hat{y})^3 + v(t - \tau), \quad (10)$$

where the adaptive gains $\hat{\delta}_1$ and $\hat{\delta}_3$ are updated according to the following adaptation laws:

$$\dot{\hat{\delta}}_1 = \theta_1 |y(t - \tau) - \hat{y}|^2, \quad \dot{\hat{\delta}}_3 = \theta_3 |y(t - \tau) - \hat{y}|^4, \quad (11)$$

where θ_1 and θ_3 are suitable positive constants to be specified by the designer. The term $v(t - \tau)$ is a feedback control in order to suppress the effects of uncertainties and is designed as follows:

$$v(t - \tau) = \hat{\eta} \text{sign}(y(t - \tau) - \hat{y}), \quad (12)$$

where

$$\text{sign}(y(t - \tau) - \hat{y}) = \begin{cases} \frac{(y(t - \tau) - \hat{y})}{|y(t - \tau) - \hat{y}|} & \text{if } y(t - \tau) - \hat{y} \neq 0 \\ 0 & \text{if } y(t - \tau) - \hat{y} = 0. \end{cases}$$

The adaptation law $\hat{\eta}$ is generated as the solution of the linear differential equation,

$$\dot{\hat{\eta}} = \varphi |y(t - \tau) - \hat{y}|, \quad (13)$$

where φ is a positive constant chosen suitably.

The proposed adaptive time-delay feedback coupling is composed of two main terms. The linear controller design is based on the empirical linear model of Pyragas²² and the nonlinear controller constructed from a locally supported basis of nonlinear control theory.^{13,16} The nonlinear term is added to compensate the perturbation of the feedback coupling. The coefficients of both terms in the feedback coupling are updated online by using a model reference adaptive control technique. Also, proposed adaptive nonlinear time-delay feedback coupling (10)–(13) will guarantee the practical synchronization of drive-response systems (3) and (8). In theory, as the adaptation gains are getting larger, the rate of parameter adaptation is getting higher. In practice, the adaptation gains are limited by the bounds of the feedback coupling and other practical considerations. One motivation of this type of feedback coupling is that it can be constructed through time varying resistors.

Now, replace t with $t - \tau$ in drive system (2), and then obtain the drive system in terms of the time-delay,

$$\dot{z}(t - \tau) = A(\alpha)z(t - \tau) + B[f(z(t - \tau), \alpha) + \xi(t - \tau)]. \quad (14)$$

For further analysis of the stability of synchronization, let us define the state synchronization error vector between the drive and the response system as $e(t) = z(t - \tau) - \hat{z}(t)$. Then, by adding and subtracting the corresponding terms, the closed-loop synchronization error dynamics is obtained as follows:

$$\begin{aligned} \dot{e} = & [A(\alpha) - LC]e + LCe + [A(\alpha) - A(\hat{\alpha})](z(t - \tau) - e) \\ & + B[f(z(t - \tau), \alpha) - f(\hat{z}, \alpha)] + B[f(\hat{z}, \alpha) - f(\hat{z}, \hat{\alpha})] \\ & - \frac{1}{2}B\hat{\delta}_1(B^TPe) - \frac{1}{2}B\hat{\delta}_3(B^TPe)^3 - B\hat{\eta} \frac{(B^TPe)}{|B^TPe|}. \end{aligned} \quad (15)$$

From the view point of control theory, the synchronization issue is equivalent to uniform stability of dynamical synchronization error system (15) at $e=0$. Then, the goal is achieved

by using the Lyapunov stability theory, whereby a positive definite energy function is chosen and its derivative is always made negative. The stability analysis of above closed-loop synchronization error dynamics (15) is given in Appendix.

The synchronization strategy is first evaluated using numerical simulation in Sec. IV.

IV. NUMERICAL RESULTS AND DISCUSSIONS

We now present results of numerical simulations to show the effectiveness of the proposed adaptive time-delay synchronization scheme and provide discussions on the robustness of the proposed adaptive time-delay synchronization scheme.

$$\begin{cases} \dot{\hat{x}}_1 = \hat{x}_2 \\ \dot{\hat{x}}_2 = -\hat{\mu}(1 + \hat{\varepsilon} \cos \omega t)\hat{x}_1 + \hat{\nu}(1 + \hat{\varepsilon} \cos \omega t)\hat{x}_2 - \hat{\beta}\hat{x}_1^3 - \hat{\gamma}\hat{x}_1^2\hat{x}_2 + \hat{\delta}_1(x_2(t-\tau) - \hat{x}_2) + \hat{\delta}_3(x_2(t-\tau) - \hat{x}_2)^3 + \hat{\eta} \operatorname{sign}(x_2(t-\tau) - \hat{x}_2), \end{cases} \quad (16)$$

with the adaptation laws,

$$\begin{aligned} \dot{\hat{\delta}}_1 &= \theta_1(x_2(t-\tau) - \hat{x}_2)^2, & \dot{\hat{\delta}}_3 &= \theta_3(x_2(t-\tau) - \hat{x}_2)^4, \\ \dot{\hat{\eta}} &= \varphi|x_2(t-\tau) - \hat{x}_2|, \end{aligned} \quad (17)$$

where θ_1 , θ_2 , and φ are three positive constants to be specified by the designer.

In the numerical simulations, the parameters of drive system (14) are as those of Fig. 1, $\varepsilon=3.392$ and $\beta=0.3$. These values were chosen according to Fig. 1, such that the system exhibits chaotic behavior and remains chaotic for slight variations of the systems parameter. However, large variation can make the system to switch to periodic or chaotic motions changing qualitatively its dynamics. In this case, the discrepancy between master and slave exponentially increases. Without loss of generality, we assume that the parameters of the drive and response systems are the same, that is, with no parameter mismatch.

Suppose the initial values of systems (14) and (A3) are, respectively, $x_1(0)=0.1$, $x_2(0)=0$, $\hat{x}_1(0)=0$, $\hat{x}_2(0)=0.1$, $\hat{\delta}_1(0)=0$, $\hat{\delta}_3(0)=0$, and $\hat{\eta}(0)=0$. Now let us set $\xi(t)=0$, $\theta_1=\theta_3=1$, $\varphi=0.01$, and $\tau=0.1$, and observe response system (A3).

The relationship between the states of the drive and response systems under the feedback coupling is depicted in Fig. 2. From this figure, it is evident that the manifolds $x_1(t-\tau)=\hat{x}_1(t)$ and $x_2(t-\tau)=\hat{x}_2(t)$ are stable. Hence, one can conclude that the chaotic oscillations of the drive and response systems are synchronized completely, so that our synchronization objective has been attained.

Figures 3(a) and 3(b) present, respectively, the time evolution of the adaptive gains $\hat{\delta}_1$ and $\hat{\delta}_3$. These results show that the estimated feedback gains $\hat{\delta}_1$, $\hat{\delta}_2$, and $\hat{\eta}$ increase with

A. Numerical simulations

We consider drive system (2) together with response system (8) and (10)–(13). The gain matrix L is chosen as $L=(0.5, 0.5)^T$ to make the transfer function,

$$H(s) = C[sI_2 - (A(\alpha) - LC)]^{-1}B = \frac{s}{s^2 + 0.4s + 0.5217},$$

be strictly positive. Then, the eigenvalues of the matrix $A(\alpha) - LC$ are $-0.2 \pm 0.6940i$

For the sake of clarity, robust adaptive response system (8) and (10)–(13) can be rewritten as follows:

time and then soon saturate at values which are optimal parameters suitable for the implementation process. It should be pointed out that when the values of the coefficients θ_1 and θ_3 of adaptation laws increase, the optimal values of the feedback gains also increase. Also, for fixed values of θ_1 and θ_3 , one can find lower values of $\hat{\delta}_1$ ($\hat{\delta}_3$) for different initial values $\hat{\delta}_1(0)$ [$\hat{\delta}_3(0)$].

In order to provide additional evidence efficiency of the proposed adaptive time-delay synchronization scheme, we plotted the parameter space considering the coefficients θ_1 and θ_3 of the adaptation laws. To characterize the degree of synchronization, we used the following error quantity:

$$\Gamma = \sqrt{(x_1(t-\tau) - \hat{x}_1(t))^2 + (x_2(t-\tau) - \hat{x}_2(t))^2},$$

where after a very long transient, we computed the average value $\langle \Gamma \rangle$ over time.

Figure 4 presents the three dimensional (3D) plot of $\langle \Gamma \rangle$ as a function of θ_1 and θ_3 when $\tau=0.1$. One can observe that the synchronous regimes are reduced by increasing θ_1 for small θ_3 . Also, desynchronous regions only exist for lower values of θ_1 and θ_3 not exceeding the value of 0.1. Hence, we find a general trend toward synchronization when increasing the coefficients of the adaptation laws.

B. Complementary roles of the linear and nonlinear terms of the feedback coupling

To understand the effects of the linear and nonlinear terms of the feedback coupling on the synchronization process, we analyze each term separately in detail.

First, we consider the drive and response systems with identical parameters. Figure 5(a) presents the 3D plot of $\langle \Gamma \rangle$ as a function of θ_1 and τ when $\theta_3=1$. This figure shows that the drive and response systems (14) and (16) are synchro-

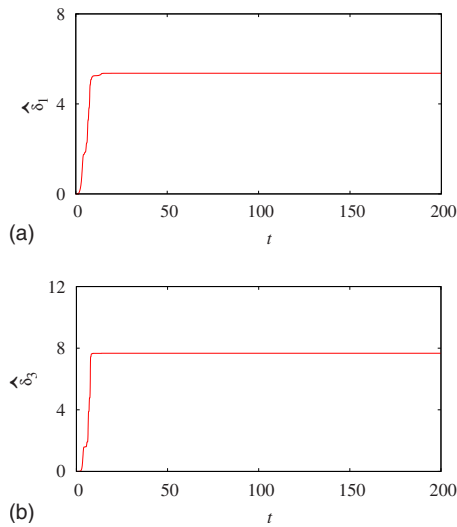


FIG. 3. (Color online) Time evolution of the adaptive gains $\hat{\delta}_1$ and $\hat{\delta}_3$ when $\tau=0.1$.

nized for small values of the time-delay τ . Note also that when the delay is greater than a critical value, increasing θ_1 does not help to improve the existence of synchronous states. Hence, a better synchronizability will probably lead to less cost in terms of the linear control coefficient.

Figure 5(b) presents the 3D plot of $\langle \Gamma \rangle$ as a function of θ_3 and τ when $\theta_1=1$. Contrary to the pattern in Fig. 5(a), Fig. 5(b) presents a general trend toward synchronization for increasing coupling strength and delay. However, we note some important differences depending on the time-delay. For a large value of θ_3 , one observes an island of unsynchronized regime in the region from $\tau \sim 0.7$ to $\tau \sim 1.2$ in spite of the fact that the coupling is strong. This can be explained by the fact that for large values of the time-delay, θ_1 is not constructive for reaching synchronization. Also, these parameters make the synchronization error system to be oscillating with a high amplitude. Generally in this case, high values of the coefficients of the adaptation laws are needed to enhance synchronization. The nonlinear term of the feedback coupling can help resolve the problem by keeping θ_1 at a low value.

To test the robustness of the proposed adaptive time-delay synchronization scheme, we performed simulations similar to those leading to Fig. 5, with 1% of mismatch on

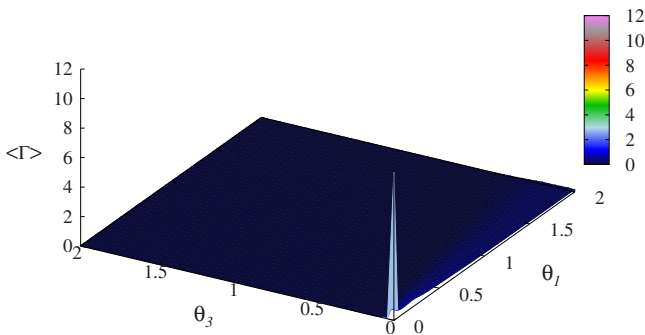


FIG. 4. (Color online) 3D plot of $\langle \Gamma \rangle$ as a function of the coefficients of the adaptation laws θ_1 and θ_3 when $\tau=0.1$.

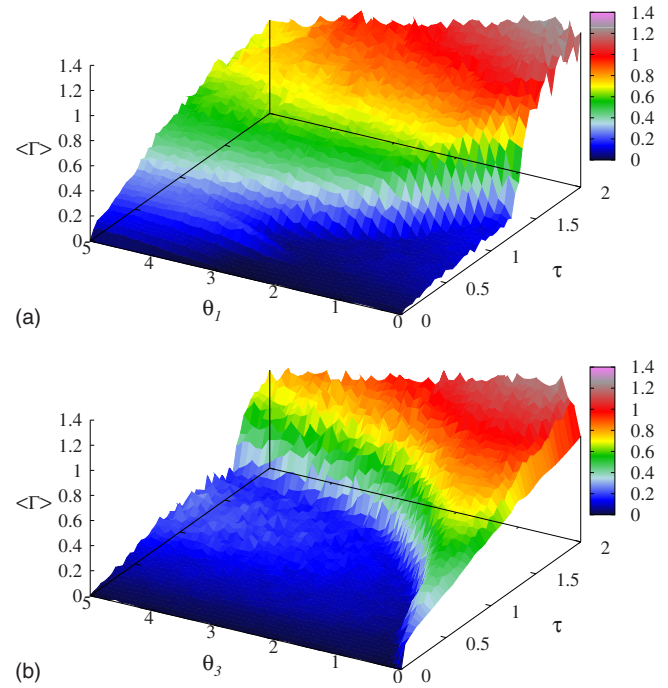


FIG. 5. (Color online) 3D plot of $\langle \Gamma \rangle$ as a function of the time-delay and (a) θ_1 and (b) θ_3 .

the parameters of the response system. The results show that the role of parameter mismatching in synchronization phenomena is quite versatile. In certain cases, the parameter mismatching is detrimental to the synchronization quality: in the case of small parameter mismatches, the synchronization error does not decay to zero with time, but can show small fluctuations around zero or even a nonzero mean value; larger values of parameter mismatching can result in the loss of complete synchronization. In some cases, parameter mismatching changes the time shift between the synchronized systems.²¹ However, in other cases their presence is necessary for synchronization. The result of our numerical simulations is presented in Fig. 6. The parameters of the response system are chosen with a difference of 1% from the parameters of the drive system. Hence, synchronization is robust with respect to mismatch. In spite of the fact that the coupling is weak, the mismatch does not change the structure of the curves compared to Figs. 5(a) and 5(b). As observed, there is a similarity between these figures.

From this analysis, we find that the linear and nonlinear terms of the feedback coupling play a complementary role in the proposed adaptive time-delay synchronization process.

To show the effectiveness of this complementary effect of the linear and nonlinear terms of the feedback coupling and to confirm the robustness with respect to parameter mismatching of the proposed synchronization algorithm, we consider the following.

Step 1: Redefine the coefficients of adaptation laws as a function of a unique parameter ϕ as $\theta_1 = \phi \tilde{\theta}_1$, $\theta_3 = \phi \tilde{\theta}_3$, and $\varphi = \phi \tilde{\varphi}$.

Step 2: Plot of the 3D graph of $\langle \Gamma \rangle$ as function of the new constant ϕ and the percentage of mismatch parameters of the response system when $\tau=0.1$.

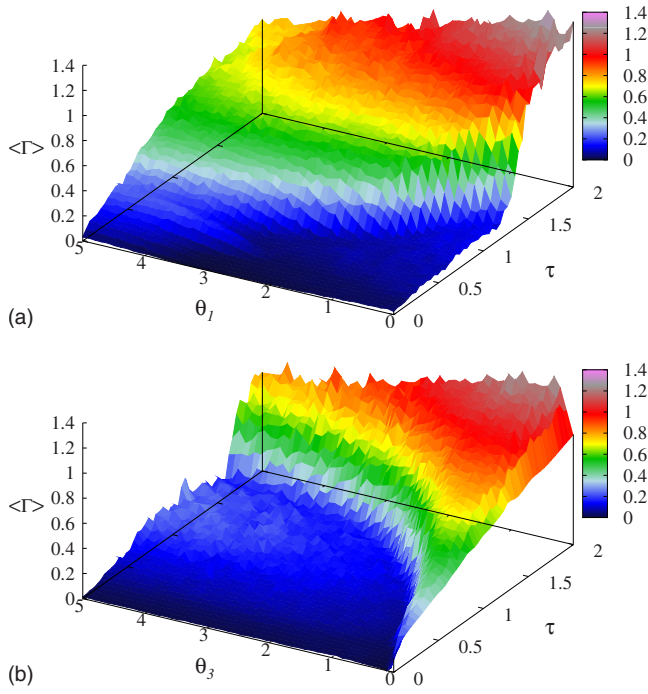


FIG. 6. (Color online) plot of $\langle \Gamma \rangle$ as a function of the time-delay τ and (a) the linear adaptive coefficient θ_1 , (b) the nonlinear adaptive coefficient θ_3 with parameters mismatching.

Figure 7 indicates the robustness of the proposed synchronization scheme with respect to parameter mismatch. The discrepancy between master and slave exponentially increases periodically with respect to the mismatch in the system due to the structure of the system and the chosen parameters as shown in Fig. 1. Although the synchronization error is higher for low values of ϕ , increasing this constant increases the rate of synchronization. Hence, the proposed synchronization scheme is robust with respect to any mismatch parameter.

Some specific questions can be posed, e.g., how much time-delays our synchronization scheme can tolerate to achieve the goal of vanishing synchronization error? Would it be possible to compensate the effect of different time-delays in the linear and nonlinear terms of the feedback coupling by increasing the magnitude of the coefficients of adaptation laws? These questions will be addressed in Sec. IV C.

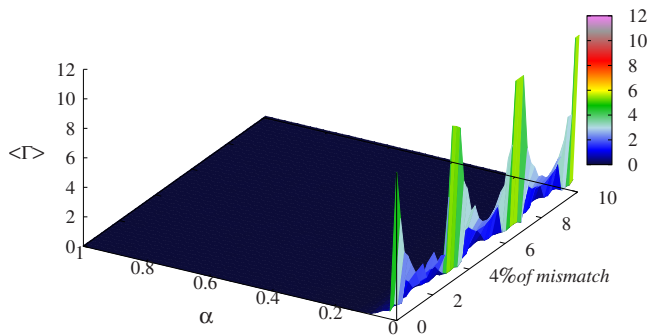


FIG. 7. (Color online) Response of the coupled systems to parameter mismatching.

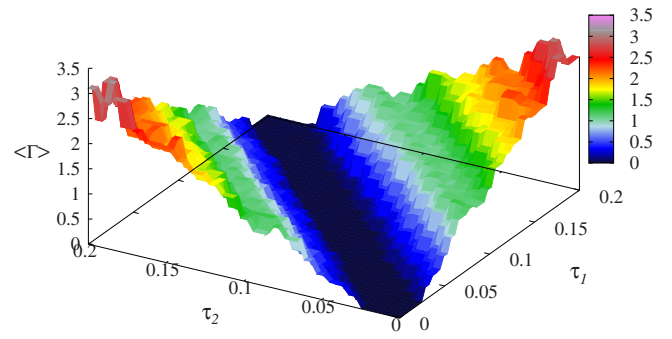


FIG. 8. (Color online) 3D plot of $\langle \Gamma \rangle$ as a function of τ_1 and τ_2 when $\theta_1 = \theta_3 = 1$ and $\varphi = 0.01$.

C. Enhancement of the coupled systems under different delays

Multifedback and multidelay systems are ubiquitous in nature and technology. Prominent examples can be found in biological and biomedical systems, laser physics, and integrated communications (see Ref. 28 and references therein). Here, we are interested in studying the behavior of two coupled DVP oscillators with different time-delays. For many technical applications, an important class of chaos control methods with time-delayed feedback have been used to synchronize chaotic systems. Contrary to most conventional multiple time-delays, the second time-delay in our work is introduced into the nonlinear term of the feedback coupling. For this purpose, we consider response system (16) and (17) with two different time-delays. The adaptive feedback coupling is chosen as follows:

$$u(t - \tau_1, t - \tau_2) = \hat{\delta}_1(x_2(t - \tau_1) - \hat{x}_2) + \hat{\delta}_3(x_2(t - \tau_2) - \hat{x}_2)^3 + \hat{\eta} \operatorname{sign}(x_2(t - \tau_1) - \hat{x}_2), \quad (18)$$

where τ_1 and τ_2 are finite time-delays, $\hat{\delta}_1$, $\hat{\delta}_3$, and $\hat{\eta}$ are solutions of the differential equations,

$$\begin{aligned} \dot{\hat{\delta}}_1 &= \theta_1(x_2(t - \tau_1) - \hat{x}_2)^2, & \dot{\hat{\delta}}_3 &= \theta_3(x_2(t - \tau_2) - \hat{x}_2)^4, \\ \dot{\hat{\eta}} &= \varphi|x_2(t - \tau_1) - \hat{x}_2|, \end{aligned} \quad (19)$$

in which θ_1 , θ_2 , and φ are three positive constants to be specified by the designer, and τ_1 and τ_2 are the two different time-delays. The same phenomenon is also observed for large values of the time-delay. Due to this fact, it is not necessary to look for the robustness of the feedback coupling with different time-delays.

Numerical simulations are depicted in Fig. 8. Our results show that complete synchronization only occurs when $\tau_1 = \tau_2$. This result is valid for large values of the time-delay. Also, when increasing the delay, the amplitudes of the oscillations increase extremely.

V. CONCLUSION

In this paper, we have studied an adaptive time-delay synchronization of a periodically modulated DVP oscillator subject to uncertainties and channel time-delay in a drive-response framework. A robust adaptive response system has

been constructed to synchronize a periodically modulated Duffing Van der Pol oscillator with unknown Lipschitz constants on function matrices, unknown bounds on uncertainties, and time-delay. Efficiency of the proposed adaptive time-delay synchronization scheme was also demonstrated through numerical simulations. They show that a coupled DVP oscillators can be synchronized through nonlinear adaptive time-delay feedback coupling. We have demonstrated that the linear and nonlinear terms in the feedback coupling play a complementary role for the improvement of the stability of the synchronization manifold. There are two main characteristics of the adaptive time-delay feedback coupling concerning the occurrence of complete synchronization.

- (i) The linear and nonlinear terms in the feedback coupling act as a combined fashion to fasten synchronization.
- (ii) The proposed adaptive time-delay synchronization is only efficient for identical time-delays in the linear and nonlinear terms in the feedback coupling.

The method applied here can be successfully applied to a large variety of physical systems. The motivation of such a choice comes from the similarity of the controlling force with a nonlinear capacitors that can be easily implemented practically using a varicap diode. However, to realize such synchronization in experiments, we have to determine the exact values of the estimated feedback gains $\hat{\delta}$ and $\hat{\eta}$. Note that the estimated feedback gains $\hat{\delta}$ and $\hat{\eta}$ are dynamical parameters and when the synchronization is accomplished, these parameters remain on constant values, which are the

optimal parameters suitable for the implementation process.

ACKNOWLEDGMENTS

F.M.M.K. thanks the PIK-Potsdam (Germany) for the partial support of this research. S.B. and D.V.S. acknowledge the support by the Alexander von Humboldt Foundation. F.M.M.K. would also like to acknowledge the partial financial support of the ICTP in Trieste-Italy under the Associate Federation Scheme. D.V.S. and J.K. acknowledge the support from EU Project No. 240763 PHOCUS(FP7-ICT-2009-C).

APPENDIX: STABILITY ANALYSIS OF THE PROPOSED ADAPTIVE TIME-DELAY SYNCHRONIZATION ALGORITHM

In this appendix, we show that the proposed adaptive time-delay synchronization scheme will guarantee practical asymptotical stability for synchronization error system (15).

Consider the Lyapunov function candidate,

$$V = e^T P e + \frac{1}{\theta_1} (\delta_1 - \hat{\delta}_1)^2 + \frac{1}{\theta_3} (\delta_3 - \hat{\delta}_3)^2 + \frac{1}{\varphi} (\eta - \hat{\eta})^2, \quad (A1)$$

where δ_1 , δ_3 , and η are positive constants to be determined later and P is a positive and symmetric matrix defined as in Eq. (6). It can easily be verified that V is a non-negative function and that it is radically unbounded, i.e., $V \rightarrow +\infty$ as $e(t)$, $(\eta - \hat{\eta})$, $(\delta_k - \hat{\delta}_k)$, $k=1, 3 \rightarrow +\infty$. The time-derivative of V along the trajectories of closed-loop system (15) satisfies

$$\begin{aligned} \dot{V} = & e^T [(A(\alpha) - LC)^T P + P(A(\alpha) - LC)] e + e^T P L C e + 2e^T P [A(\alpha) - A(\hat{\alpha})] (z(t - \tau) - e) + 2e^T P B [f(z(t - \tau), \alpha) - f(\hat{z}, \alpha)] \\ & + 2e^T P B [f(\hat{z}, \alpha) - f(\hat{z}, \hat{\alpha})] + 2e^T P B \xi(t - \tau) - 2\hat{\delta}_1 |B^T P e|^2 - 2\hat{\delta}_3 |B^T P e|^4 - \hat{\eta} |B^T P e| \\ & - \frac{2}{\theta_1} (\delta_1 - \hat{\delta}_1) \dot{\hat{\delta}}_1 - \frac{2}{\theta_3} (\delta_3 - \hat{\delta}_3) \dot{\hat{\delta}}_3 - \frac{2}{\varphi} (\eta - \hat{\eta}) \dot{\hat{\eta}}, \\ \leq & -e^T Q e + 2k_a \lambda_{\max}(P) \|\alpha - \hat{\alpha}\| \|e\| (\|e\| + \|z(t - \tau)\|) + 2k_{f_1} |B^T P e| + 2k_{f_3} |B^T P e|^3 + 2\|L^T P\| \|e\| |B^T P e| + 2(\phi_m + \xi_m) |B^T P e| \\ & - 2\hat{\delta}_1 |B^T P e|^2 - 2\hat{\delta}_3 |B^T P e|^4 - 2\hat{\eta} |B^T P e| - \frac{2}{\theta_1} (\delta_1 - \hat{\delta}_1) \dot{\hat{\delta}}_1 - \frac{2}{\theta_3} (\delta_3 - \hat{\delta}_3) \dot{\hat{\delta}}_3 - \frac{2}{\varphi} (\eta - \hat{\eta}) \dot{\hat{\eta}}. \end{aligned} \quad (A2)$$

Now, let $\Delta\alpha_m = \|\alpha - \hat{\alpha}\|$. Since trajectories of system (2) are contained in an attractor, we can suppose that $\|z(t - \tau)\| \leq r$ for some $r > 0$. Moreover, we can also suppose that there exists $r > 0$ large enough, such that whole synchronization error system (15) is contained in the domain $\Sigma = \{e \in R^2, \|e\| \leq 2r, r > 0\} \subset \mathcal{M}$. Then, one has

$$\begin{aligned} \dot{V} \leq & -e^T Q e + 12k_a r^2 \lambda_{\max}(P) \Delta\alpha_m + 2k_{f_1} |B^T P e| \\ & + 2k_{f_3} |B^T P e|^3 + 4r \|L^T P\| |B^T P e| + 2(\phi_m + \xi_m) |B^T P e|. \end{aligned} \quad (A3)$$

Now, let

$$\delta_1 = k_{f_1}, \quad \delta_3 = k_{f_3}, \quad \eta = \phi_m + \xi_m + 2r \|L^T P\| \quad \text{and}$$

$$\zeta = 12k_a r^2 \lambda_{\max}(P) \Delta\alpha_m. \quad (A4)$$

Using adaptation laws (11) and (13), one finally gets

$$\dot{V} \leq -\lambda_{\min}(Q) \|e\|^2 + \zeta, \quad (A5)$$

where $\lambda_{\min}(Q)$ is the minimum eigenvalue of Q . Then, from Eq. (A1), it follows that if

$$\|e(t)\| > \sqrt{\frac{\zeta}{\lambda_{\min}(Q)}},$$

then $\dot{V} < 0$. Hence V decreases, which implies that $\|e\|$ decreases as well [see Eq. (A1)]. It then follows from standard invariance arguments that asymptotically the error satisfies the following bound:

$$\|e(t)\| \leq c, \quad (\text{A6})$$

where $c \geq \sqrt{\zeta/\lambda_{\min}(Q)}$ (see, e.g., Refs. 13, 16, and 17).

From Eq. (A2), one can see that the asymptotic error depends linearly on the free parameter ζ . Hence, if this parameter is small, the resulting error will be small as well. The dependence of the error on $\Delta\alpha_m$ deserves special attention. Note that $\zeta = 12k_a r^2 \lambda_{\max}(P) \Delta\alpha_m$. Hence as $\Delta\alpha_m$ decreases, ζ will increase, which decreases the asymptotic error bound. This argument shows that with the proposed synchronization method, $\Delta\alpha_m$ should be made as small as possible. Therefore, the state error would be contained within a neighborhood of the origin. Note that if $\Delta\alpha_m = 0$, i.e., $\alpha = \hat{\alpha}$ (so that $\zeta = 0$), the synchronization error system is globally asymptotically synchronized on \mathcal{M} .

¹A. Pikovsky, M. Rosenblum, and J. Kurths, *Synchronization: A Universal Concept in Nonlinear Sciences* (Cambridge University Press, Cambridge, 2001).

²S. Boccaletti, J. Kurths, G. Osipov, D. L. Valladares, and C. Zhou, *Phys. Rep.* **366**, 1 (2002).

³P. So, B. C. Cotton, and E. Barreto, *Chaos* **18**, 037114 (2008).

⁴A. Koseska, E. Volkov, and J. Kurths, *Chaos* **20**, 023132 (2010).

⁵H. Ulrichs, A. Mann, and U. Parlitz, *Chaos* **19**, 043120 (2009).

⁶Y. Sun and J. Ruan, *Chaos* **19**, 043113 (2009).

⁷F. Sorrentino, G. Barlev, A. B. Cohen, and E. Ott, *Chaos* **20**, 013103 (2010).

⁸S. Bowong and F. M. Moukam Kakmeni, *Phys. Lett. A* **316**, 206 (2003).

⁹F. M. Moukam Kakmeni, S. Bowong, C. Tchawoua, and E. Kaptouom, *Phys. Lett. A* **322**, 305 (2004).

¹⁰L. Wang, H. P. Dai, H. Dong, Y. Y. Cao, and Y. X. Sun, *Eur. Phys. J. B* **61**, 335 (2008).

¹¹V. Volterra, *Leçons sur la Théorie Mathématique de la Lutte Pour la Vie* (Gauthiers-Villars, Paris, 1931).

¹²F. Ghiringhelli and M. N. Zervas, *Phys. Rev. E* **65**, 036604 (2002); F. M. Atay, *Phys. Rev. Lett.* **91**, 094101 (2003).

¹³H. K. Khalil, *Nonlinear Systems*, 3rd ed. (Springer-Verlag, London, 1995).

¹⁴D. V. Senthilkumar, M. Lakshmanan, and J. Kurths, *Phys. Rev. E* **74**, 035205(R) (2006).

¹⁵D. V. Senthilkumar, J. Kurths, and M. Lakshmanan, *Phys. Rev. E* **79**, 066208 (2008).

¹⁶F. M. Moukam Kakmeni, S. Bowong, and C. Tchawoua, *Phys. Lett. A* **355**, 47 (2006).

¹⁷M. Chen, D. Zhou, and Y. Shang, *Phys. Lett. A* **337**, 384 (2005).

¹⁸H. N. Pishkenari, N. Jalili, S. H. Mahboobi, A. Alasty, and A. Meghdari, *Chaos* **20**, 023105 (2010).

¹⁹M. Dhamala, V. K. Jirsa, and M. Ding, *Phys. Rev. Lett.* **92**, 074104 (2004).

²⁰V. M. Popov, *Hyperstability of Control System* (Springer-Verlag, Berlin, 1973).

²¹E. M. Shahverdiev, R. A. Nuriev, R. H. Hashimov, and K. A. Shore, *Chaos, Solitons Fractals* **25**, 325 (2005).

²²K. Pyragas, *Phys. Lett. A* **170**, 421 (1992).

²³F. M. Moukam Kakmeni, S. Bowong, L. Nana, and T. C. Kofane, *Chaos, Solitons Fractals* **39**, 248 (2009).

²⁴M. A. Trevisan, J. M. Mendez, and G. B. Mindlin, *Phys. Rev. E* **73**, 061911 (2006).

²⁵T. Gardner, G. Cecchi, M. Magnasco, R. Laje, and G. B. Mindlin, *Phys. Rev. Lett.* **87**, 208101 (2001).

²⁶R. Laje, T. J. Gardner, and G. B. Mindlin, *Phys. Rev. E* **65**, 051921 (2002).

²⁷E. J. Ngamga Ketchamen, L. Nana, and T. C. Kofane, *Chaos, Solitons Fractals* **20**, 1141 (2004).

²⁸A. Ahlborn and U. Parlitz, *Phys. Rev. Lett.* **93**, 264101 (2004); *Phys. Rev. E* **75**, 065202(R) (2007); *Opt. Lett.* **31**, 465 (2006).